Noname manuscript No.
(will be inserted by the editor)

State Estimation of Mobile Robot using GPS Signal that Includes Reflected and Diffracted Waves

Takeshi Nishida · Sozo Inoue · Shinichi Sagara

Received: date / Accepted: date

Abstract We propose a method to improve the state estimation accuracy of mobile robots placed near high-rise buildings using the statistical property of the reflected and diffracted waves of GPS (global positioning system) signals. First, it is assumed that a GPS signal that contains a reflected and diffracted wave is denoted by the sum of the true position information and noise that follows a time-varying Gaussian distribution. On the basis of this assumption, the time-varying bias of a GPS signal is tracked using a Kalman filter. In addition, a particle filter, which executes sampling and likelihood evaluation using the estimated bias, is developed. With the proposed method, a GPS signal that contains the rejected noise introduced by the conventional method can be used efficiently, and the state estimation accuracy of the robot in a shadow area of GPS satellite can be improved. Furthermore, a control system for an autonomous mobile robot incorporating the proposed state estimation mechanism is developed, and its effectiveness is evaluated via simulation.

Keywords GPS · reflected and diffracted waves · particle filter · vehicle control

1 Introduction

GPS (global positioning system) is widely used for the self-localization of outdoor mobile robot. Theoretically, if there are four or more GPS satellites that can carry out signal reception directly using the antenna with which the robot is equipped, position measurement is possible[1]; the positioning quality can be improved via reception from more visible satellites[2] . In general, the GPS satellite that can carry out signal reception directly is called a visible satellite and other satellites are called invisible satellites. Moreover, an area where a required number of visible satellites are not available is called a shadow area. The measurement error of GPS becomes significant because shadow areas occur where many high-rise buildings exist around a robot, as shown in Fig.1[1].

The most general method for solving this problem is the state estimation method using dead reckoning and map information; this method is widely used in vehicle navigation systems[3]. In this technique, the direct wave from a visible satellite and the reflected wave and diffracted wave from an invisible satellite are classified first[4]. When the signal from a sufficient number of visible satellites is not acquired, the use of GPS signal ceases, and dead reckoning based on odometry and map information is adopted. However, since dead reckoning has the drawback of signal accumulation errors with no means to eliminate it, prolonged use is difficult[5].

In contrast, a GPS measurement method using a three-dimensional map is proposed[2]. In this method, visible and invisible GPS satellites are identified using a city area map that has height direction information. Furthermore, the state variables of a robot in a shadow area are estimated using a PF (particle filter) [6,7]. However, it is necessary to compute the shadow areas using the three-dimensional map information and the direction of GPS satellites, and therefore, it is difficult to apply this method to a place for which no three-dimensional map is available.

Thus, we propose a method for improving a mobile robot's state estimation accuracy using the statistical character of the reflected and diffracted waves of a GPS signal. First, it is assumed that a GPS signal that contains reflected and diffracted waves is represented by

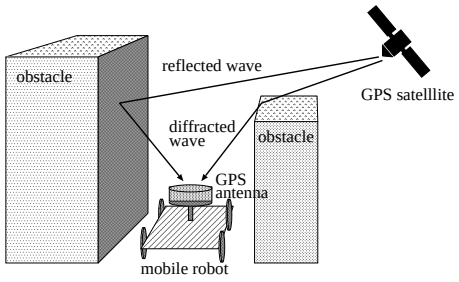

Fig. 1 GPS signal from an invisible satellite.

true position information and the sum of the noise that follows a time-varying Gaussian distribution. Based on this assumption, the time-varying bias of the Gaussian distribution is estimated using a KF (Kalman filter), and a PF, which executes sampling and likelihood evaluation using the estimated bias, are developed. According to this state estimation mechanism, a GPS signal is effectively used and the state estimation accuracy of a robot in the shadow area is improved. Furthermore, the control system of an autonomous mobile robot incorporating the proposed state estimation method is developed.

The remainder of this paper is organized as follows: Section 2 presents the probabilistic model of a mobile robot. In Section 3, a state estimation method using a PF and a feedback control method is proposed. In Section 4, the performance of the proposed methods is verified via simulation. Finally, Section 5 provides a summary of the paper.

2 Probabilistic Model of a Mobile Robot

2.1 Kinematic Model

Let a front-wheel-steering rear-wheel-drive-type four-wheel mobile robot be a controlled object in this paper. Because the driving wheel of the robot is a differential type, the rear wheel dose not slide during rotational movement. The robot's state variables are defined by the position and angle in the inertial reference system $O-XY$.

$$\boldsymbol{x}_k \triangleq [x_k\ y_k\ \theta_k]^T = [\boldsymbol{z}_k^T\ \theta_k]^T \tag{1}$$

where $k = 0, 1, 2, \cdots$ is discrete time, $\boldsymbol{z}_k \triangleq [x_k\ y_k]^T$ is the center position of the robot based on the center of the rear wheel axle, θ_k is the angle between the robot's direction of movement and the X axis, and l is the length of the wheel base. Next, the motion reference input is defined as

$$\boldsymbol{u}_k \triangleq [v_k\ \phi_k]^T, \tag{2}$$

where v_k denotes the direction of movement speed, which occurs because the driving wheel and ϕ_k denotes the steering angle of the front wheel, which makes a positive counterclockwise rotation. The relation of these parameters and the coordinate systems is shown in Fig.2

When it is assumed that skidding does not occur, the discrete time state equation of the mobile robot can be expressed as follows [3]:

$$\begin{aligned}\boldsymbol{x}_{k+1} &= \boldsymbol{f}(\boldsymbol{x}_k, \boldsymbol{u}_k) \\ &= \boldsymbol{x}_k + \begin{bmatrix} \frac{v_k}{\omega_k}\{\sin(\theta_k + \omega_k \Delta) - \sin\theta_k\} \\ -\frac{v_k}{\omega_k}\{\cos(\theta_k + \omega_k \Delta) - \cos\theta_k\} \\ \omega_k \Delta \end{bmatrix},\end{aligned} \tag{3}$$

where

$$\omega_k \triangleq (v_k/l)\tan\phi_k \tag{4}$$

and Δ is the sampling time.

2.2 Probabilistic Discrete State Space Model

In an actual robot system, some noise may merge with the control input under the influence of backlash/degradation of the drive system or an uneven road surface, etc. Therefore, we assume that the disturbance according to a normal distribution merges with the command input of Eq.(2) and the control input is modeled as follows[3]:

$$\hat{v}_k \triangleq v_k + \varepsilon_v, \quad \varepsilon_v \sim \mathcal{N}(0, \alpha_1 v_k^2 + \alpha_2 \phi_k^2) \tag{5}$$

$$\hat{\phi}_k \triangleq \phi_k + \varepsilon_\phi, \quad \varepsilon_\phi \sim \mathcal{N}(0, \alpha_3 v_k^2 + \alpha_4 \phi_k^2), \tag{6}$$

where α_i $(i = 1, 2, 3, 4)$ is a positive constant that determines the characteristic of the noise. In a similar manner, considering the disturbance added in the direction of the robot by road surface unevenness etc., the transition of the angle of direction is modeled as follows:

$$\hat{\theta}_{k+1} = \hat{\theta}_k + (\hat{\omega}_k + \varepsilon_\gamma)\Delta,\ \varepsilon_\gamma \sim \mathcal{N}(0, \alpha_5 v_k^2 + \alpha_6 \phi_k^2), \tag{7}$$

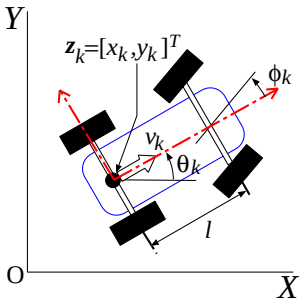

Fig. 2 State of a mobile robot in the world coordinate system.

where $\hat{\omega}_k \triangleq (\hat{v}_k/l)\tan\hat{\phi}_k$ and α_j $(j = 5, 6)$ is the positive constant that determines the characteristic of the noise. For simplification, the noises are described as $\boldsymbol{\varepsilon}_k \triangleq [\varepsilon_v \ \varepsilon_\phi \ \varepsilon_\gamma]^T$.

From the above relations, Eq. (3) can be described as a probabilistic discrete state model as follows:

$$\hat{\boldsymbol{x}}_{k+1} = \hat{\boldsymbol{x}}_k + \begin{bmatrix} \frac{\hat{v}_k}{\hat{\omega}_k}\left\{\sin(\hat{\theta}_k + \hat{\omega}_k\Delta) - \sin\hat{\theta}_k\right\} \\ -\frac{\hat{v}_k}{\hat{\omega}_k}\left\{\cos(\hat{\theta}_k + \hat{\omega}_k\Delta) - \cos\hat{\theta}_k\right\} \\ (\hat{\omega}_k + \varepsilon_\gamma)\Delta \end{bmatrix} \sim p_f\left(\hat{\boldsymbol{x}}_{k+1}\middle|\hat{\boldsymbol{x}}_k, \boldsymbol{u}_k\right), \tag{8}$$

where $\hat{\boldsymbol{x}}_k \triangleq [\hat{x}_k \ \ \hat{y}_k \ \ \hat{\theta}_k]^T$ denotes the state variables containing the probabilistic elements.

2.3 Observation Model

The mobile robot observes the self-position $\boldsymbol{z}_k^{\mathrm{GPS}} \triangleq [x_k^{\mathrm{GPS}} \ y_k^{\mathrm{GPS}}]^T$ at each discrete time interval using the provided GPS antenna as follows:

$$\boldsymbol{z}_k^{\mathrm{GPS}} = \boldsymbol{z}_k + \boldsymbol{\xi}_k, \tag{9}$$

where

$$\boldsymbol{\xi}_k \sim \begin{cases} \mathcal{N}(r_k, \boldsymbol{\Sigma}_s) & \text{if the robot is in a shadow area,} \\ \mathcal{N}(0, \boldsymbol{\Sigma}_b) & \text{otherwise,} \end{cases} \tag{10}$$

and r_k denotes the time-varying bias of the Gaussian distribution. Thus, $\boldsymbol{\xi}_k$ is a noise vector according to the time-varying normal distribution from which its bias and variance change with respect to the environment around of the robot. Here, the covariance matrices are $\boldsymbol{\Sigma}_s = \mathrm{diag}[\sigma_s^2, \sigma_s^2]$ and $\boldsymbol{\Sigma}_b = \mathrm{diag}[\sigma_b^2, \sigma_b^2]$. In general, because the distribution in the shadow area becomes larger than that of a direct wave, the condition

$$\det(\boldsymbol{\Sigma}_b) < \det(\boldsymbol{\Sigma}_s) \tag{11}$$

is fulfilled.

Next, the measurement of direction is not included in a GPS signal, and therefore, it is calculated from the robot's direction as follows:

$$\theta_k^{\mathrm{GPS}} = \tan^{-1}\left(\frac{y_k^{\mathrm{GPS}} - \hat{y}_{k-1}}{x_k^{\mathrm{GPS}} - \hat{x}_{k-1}}\right) + \omega_{k-1}\Delta. \tag{12}$$

An observation vector consists of these observed values as follows:

$$\boldsymbol{h}(\hat{\boldsymbol{x}}_k) = \boldsymbol{y}_k^{\mathrm{GPS}} \triangleq \left[x_k^{\mathrm{GPS}} \ y_k^{\mathrm{GPS}} \ \theta_k^{\mathrm{GPS}}\right]^T. \tag{13}$$

3 State Estimation and Control

3.1 Control System Including Particle Filter

The state variable diagram of the robot control system developed in this research is shown in Fig.3. This control system is developed for the robot which passes through the specified domain by controlling only the steering angle under the speed regularity of the robot. In this control system, the state transition of the robot is represented using a nonlinear model and the noise according to the time-varying Gaussian distribution is added to the observed signal. The PF executes three steps, i.e., sampling, likelihood evaluation, and resampling, and it functions as a state observer.

In many conventional researches that estimate state variables of a mobile robot using a PF and a GPS signal, the sampling procedure is executed based on a kinematic model and likelihood evaluation is executed based on the GPS signal. When such a procedure is employed, the situation where a difference of prediction (i.e., the sampling) and observation (i.e., the likelihood evaluation) suddenly becomes significant, the estimation is executed only in the domain where many particles exist, i.e., the domain where the sampling according to the kinematic model had been executed and the sudden change of observation is disregarded. This situation works effectively when the bias of a GPS signal returns to 0 after a short time. However, the estimation error of a kinematics model accumulates with time. Moreover, when the resampling procedure is executed in such a situation, state estimation jumps discontinuously to the observation domain of the GPS signal because the particles may move suddenly, resulting in the feedback control system becoming unstable. Therefore, when the changes in the bias and variance of the noise in the GPS signal are large, in order to continue driving a control system stably, it is necessary to include the statistical characteristics of the GPS signal in the shadow area in a state estimator as prior knowledge. Then, in order

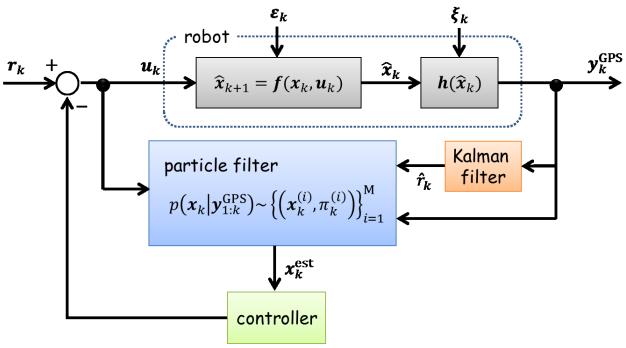

Fig. 3 State variable diagram with PF observer.

to estimate the bias of the GPS signal, first, a KF is employed. Next, the state estimation of the robot is executed using the bias estimated by the KF, and the PF incorporates the statistical characteristics of the noise of the GPS signal as prior knowledge. Then, the control input is calculated via PF using the estimation.

3.2 Bias Estimation by Kalman Filter

The output modeled by Eq. (10) is represented as a system including the noise following a Gaussian distribution as follows:

$$\boldsymbol{\eta}_{k+1} = \boldsymbol{A}\boldsymbol{\eta}_k, \tag{14}$$

$$\boldsymbol{z}_k^{\mathrm{GPS}} = \boldsymbol{C}\boldsymbol{\eta}_k + \boldsymbol{w}_k, \tag{15}$$

where

$$\boldsymbol{\eta}_k \triangleq \begin{bmatrix} \hat{x}_k \\ \hat{v}_{xk} \\ \hat{y}_k \\ \hat{v}_{yk} \end{bmatrix}, \ \boldsymbol{A} \triangleq \begin{bmatrix} 1 & \Delta & 0 & 0 \\ 0 & 1 & 0 & 0 \\ 0 & 0 & 1 & \Delta \\ 0 & 0 & 0 & 1 \end{bmatrix}, \ \boldsymbol{C} \triangleq \begin{bmatrix} 1 & 0 \\ 0 & 0 \\ 0 & 1 \\ 0 & 0 \end{bmatrix}$$

$$\boldsymbol{w}_k \sim \mathcal{N}(\boldsymbol{0}, \boldsymbol{R}), \quad \boldsymbol{R} \triangleq \mathrm{diag}\left[\sigma_c^2 \ \sigma_c^2\right],$$

and $\hat{v}_{xk}$ and $\hat{v}_{yk}$ are velocities of the X- and Y-axis orientations, respectively, and σ_c^2 is a covariance matrix of $\boldsymbol{w}_k$. A KF is applied to this system to remove the noise according to a Gaussian distribution as follows:

$$\boldsymbol{\eta}_k^- = \boldsymbol{A}\boldsymbol{\eta}_{k-1} \tag{16}$$

$$\boldsymbol{P}_k^- = \boldsymbol{A}\boldsymbol{P}_{k-1}\boldsymbol{A}^T \tag{17}$$

$$\boldsymbol{K}_k^- = \boldsymbol{P}_k^-\boldsymbol{C}^T\left(\boldsymbol{C}\boldsymbol{P}_k^-\boldsymbol{C}^T + \boldsymbol{R}\right)^{-1} \tag{18}$$

$$\boldsymbol{\eta}_k = \boldsymbol{\eta}_k^- + \boldsymbol{K}_k\left(\boldsymbol{z}_k^{\mathrm{GPS}} - \boldsymbol{C}^T\boldsymbol{\eta}_k^-\right) \tag{19}$$

$$\boldsymbol{P}_k = \left(\boldsymbol{I} - \boldsymbol{K}_k\boldsymbol{C}\right)\boldsymbol{P}_k^- \tag{20}$$

Here, in order to take into consideration the noise according to a larger distribution, we set the variance as $\sigma_c^2 = \sigma_s^2$ based on the assumption of Eq. (11).

The bias of a GPS signal is estimated using $\boldsymbol{\eta}_k$, which is estimated using the above Kalman filter as follows:

$$\hat{r}_k = \sqrt{\hat{x}_k^2 + \hat{y}_k^2} \tag{21}$$

3.3 Sampling

The PF executes state estimation using a set of M particles with weight $\left\{\boldsymbol{x}_k^{(i)}, \pi_k^{(i)}\right\}_{i=1}^{M}$. Here, $\boldsymbol{x}_k^{(i)}$ is the position of the particles in the state space and $\pi_k^{(i)} \geq 0$ represents the weight of each particle. Subsequently, sampling, which is one of the estimation procedures using the PF, is described in detail.

In this research, the proposal distribution for movement of particles and distribution is designed as follows:

$$\tilde{\boldsymbol{x}}_k^{(i)} \sim p_q\left(\tilde{\boldsymbol{x}}_k^{(i)} | \boldsymbol{x}_{k-1}^{(i)}\right) = \begin{cases} p_f\left(\tilde{\boldsymbol{x}}_k^{(i)} | \boldsymbol{x}_{k-1}^{(i)}\right) & (95\% \text{ of particles}), \\ p_r\left(\tilde{\boldsymbol{x}}_k^{(i)} | \boldsymbol{x}_{k-1}^{(i)}\right) & (5\% \text{ of particles}). \end{cases} \tag{22}$$

In this procedure, function $p_f(\cdot)$ executes sampling for 95% of the particle set in consideration of the particle distribution, the previous input, and system noise. This is the sampling function of the general PF and it is used by many conventional researches [8]. However, when movement in the shadow area continues for a long time, the estimated error accumulates and the control drive system becomes unstable.

In contrast, 5% of particles chosen at random are executed using sampling according to the function $p_r(\cdot)$ as shown below:

$$\boldsymbol{x}_k^{(i)} = \boldsymbol{f}\left(\boldsymbol{x}_{k-1}^{\mathrm{est}}, \boldsymbol{u}_{k-1}\right) + \boldsymbol{R}_\psi\boldsymbol{\rho}(\hat{r}_k) \sim p_r\left(\boldsymbol{x}_k^{(i)} | \boldsymbol{x}_{k-1}^{(i)}\right), \tag{23}$$

where $\boldsymbol{x}_{k-1}^{\mathrm{est}}$ is the latest posteriori estimate,

$$\boldsymbol{\rho}(\hat{r}_k) \triangleq [\rho(\hat{r}_k) \ \ 0]^T, \quad \rho(\hat{r}_k) \sim \mathcal{N}\left(\hat{r}_s, \sigma_b^2\right), \tag{24}$$

$$\boldsymbol{R}_\psi \triangleq \begin{bmatrix} \cos\psi & -\sin\psi \\ \sin\psi & \cos\psi \end{bmatrix}, \quad \psi \in \mathrm{rand}[-\pi, \pi]. \tag{25}$$

Moreover, the weight of particles sampled by $p_q(\cdot)$ is given as follows:

$$\pi_k^{(i)} = \frac{1}{M\sqrt{2\pi\sigma_s^2}} \exp\left\{-\frac{1}{2}\frac{\rho(\hat{r}_k)^2}{\sigma_s^2}\right\} \tag{26}$$

First, the particles are sampled on the basis of the state values estimated using the kinematic model shown in Eq. (3) according to the Gaussian distribution $\mathcal{N}\left(\hat{r}_k, \sigma_b^2\right)$. Then, random rotational coordinate transformations with radius $\hat{r}_k$ are executed on the particles. This is a contrivance to improve the accuracy of state estimation, and which enables it to use the GPS signal in the shadow area. The assumptions expressed in Eq. (9) and (10) are represented as $p_r(\cdot)$ and installed into the procedure of the PF. The outline of these sampling methods is shown in Fig.4.

3.4 Likelihood Evaluation

The likelihood function based on the GPS signal in the area that receives the signals from a GPS satellite di-

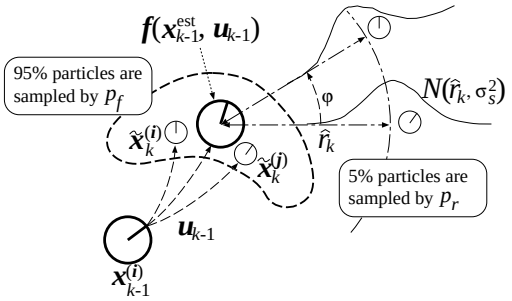

Fig. 4 Overview of the proposed sampling procedure.

rectly is given as follows:

$$p_{\text{direct}}\left(\boldsymbol{y}_k^{\text{GPS}}|\boldsymbol{x}_k^{(i)}\right) = \frac{2}{3}\cdot\frac{1}{2\pi\sigma_b^2}\left\{\exp\left(-\frac{d_x^2}{2\sigma_b^2}\right)+\exp\left(-\frac{d_y^2}{2\sigma_b^2}\right)\right\} + \frac{1}{3}\cdot\frac{1}{2\pi\sigma_p^2}\exp\left(-\frac{d_\theta^2}{2\sigma_p^2}\right), \tag{27}$$

where

$$d_x = \delta\left(x_k^{(i)} - x_k^{\text{GPS}}\right), \tag{28}$$

$$d_y = \delta\left(y_k^{(i)} - y_k^{\text{GPS}}\right), \tag{29}$$

$$d_\theta = \delta\left(\theta_k^{(i)} - \theta_k^{\text{GPS}}\right), \tag{30}$$

and $\delta(\cdot)$ is the Dirac delta function. Furthermore, the likelihood function based on the GPS signal in the shadow area is given as follows:

$$p_{\text{shadow}}\left(\boldsymbol{y}_k^{\text{GPS}}|\boldsymbol{x}_k^{(i)}\right) = \frac{2}{3}\cdot\frac{1}{2\pi\sigma_s^2}\exp\left(-\frac{d_{xy}^2}{2\sigma_s^2}\right)+\frac{1}{3}\cdot\frac{1}{2\pi\sigma_p^2}\exp\left(-\frac{d_\theta^2}{2\sigma_p^2}\right), \tag{31}$$

where

$$d_{xy} = |\delta(z_k^{(i)} - z_k^{\text{GPS}})| - \hat{r}_k. \tag{32}$$

The observation model of the PF is constructed by composition of these likelihood function as follows:

$$p_h\left(\boldsymbol{y}_k^{\text{GPS}}|\boldsymbol{x}_k^{(i)}\right) = \frac{1}{2}p_{\text{direct}}\left(\boldsymbol{y}_k^{\text{GPS}}|\boldsymbol{x}_k^{(i)}\right)+\frac{1}{2}p_{\text{shadow}}\left(\boldsymbol{y}_k^{\text{GPS}}|\boldsymbol{x}_k^{(i)}\right). \tag{33}$$

The outline of this likelihood function is shown in Fig.5.

The weight $\tilde{\pi}_k^{(i)}$ of particle $\tilde{\boldsymbol{x}}_k^{(i)}$ is updated using this likelihood function as follows:

$$\tilde{\pi}_k^{(i)} \propto \pi_{k-1}^{(i)} p_h\left(\boldsymbol{y}_k^{\text{GPS}}|\boldsymbol{x}_k^{(i)}\right), \quad (\forall i), \tag{34}$$

where all the weights are normalized so that $\sum_{i=1}^{M}\tilde{\pi}_k^{(i)} = 1$ after updating.

A posteriori estimation of the PF can be computed after likelihood evaluation as follows:

$$\boldsymbol{x}_k^{\text{est}} = \sum_{i=1}^{M}\pi_k^{(i)}\delta(\boldsymbol{x}_k^{(i)}) \tag{35}$$

Furthermore, a control input is drawn using this posteriori estimation [9] as follows:

$$\phi_k k + 1 = k_\phi\left(\phi_k^* \ominus \phi_k\right), \tag{36}$$

$$v_k = \text{const.}, \tag{37}$$

where

$$\phi_k^* = \tan^{-1}\frac{y_i^{\text{target}} - y_k^{\text{est}}}{x_i^{\text{target}} - x_k^{\text{est}}}, \tag{38}$$

$\phi^*, \phi \in [0, 2\pi)$, $\ominus$ denotes the smallest angular difference on a circle, and k_ϕ denotes the feedback gain.

3.5 Resampling

Execution of resampling is dependent on the ESS (effective sample size) [10]:

$$ESS = \frac{1}{\sum_{i=1}^{M}\left(\tilde{\pi}_k^{(i)}\right)^2}. \tag{39}$$

$ESS = M$ when the weight of all the particles is equal and when the variety of weights is the largest, $ESS = 1$. This value is an indicator of the number of particles currently utilized effectively and it is introduced in order to control the frequent occurrence of resampling. An appropriate threshold ESS_{th} is prepared and resampling is executed if the obtained ESS is less than ESS_{th}.

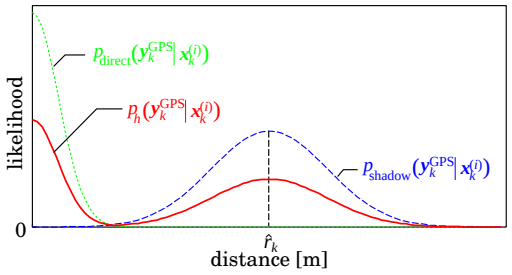

Fig. 5 Likelihood function of a measurement model.

Resampling of $\boldsymbol{x}_k^{(i)}$ is carried out by the probability of $\tilde{\pi}_k^{(i)}$ as follows:

$$\boldsymbol{x}_k^{(i)} \sim \begin{cases} \tilde{\boldsymbol{x}}_k^{(1)} & \text{with prob. } \tilde{\pi}_k^{(1)} \\ \vdots & \vdots \\ \tilde{\boldsymbol{x}}_k^{(M)} & \text{with prob. } \tilde{\pi}_k^{(M)} \end{cases}, \quad (\forall i) \tag{40}$$

Then, the weights are normalized as follows:

$$\pi_k^{(i)} := 1/M, \ (\forall i), \tag{41}$$

where ":=" denotes substitution. When resampling is not carried out, the following is executed:

$$\boldsymbol{x}_k^{(i)} := \tilde{\boldsymbol{x}}_k^{(i)}, \quad \pi_k^{(i)} := \tilde{\pi}_k^{(i)}. \tag{42}$$

From these procedures, a new set of particles

$$\left\{ \left(\boldsymbol{x}_k^{(m)}, \pi_k^{(m)} \right) \right\}_{m=1}^{M} \sim p(\boldsymbol{x}_k | \boldsymbol{y}_{1:k}), \tag{43}$$

is constructed. Then, the sampling is repeated with $k := k+1$. The procedure of PF described above is shown in Algorithm 1.

4 Simulation

The numerical simulation presented below shows that appropriate state estimation is achieved and continued using the proposed method even in the shadow area.

Algorithm 1 Particle Filter

loop
  for $i := 1$ to M **do**
    $\tilde{\boldsymbol{x}}_k^{(i)} \sim p_q(\cdot | \boldsymbol{x}_{k-1}^{\text{est}})$
  end for
  for $i := 1$ to M **do**
    $\tilde{\pi}_k^{(i)} \propto \tilde{\pi}_{k-1}^{(i)} \cdot p_h\left(\boldsymbol{y}_k^{\text{GPS}} | \boldsymbol{x}_k^{(i)} \right)$
  end for
  calculation of $\boldsymbol{x}_k^{\text{est}} = \sum_{i=1}^{M} \pi_k^{(i)} \delta(\boldsymbol{x}_k^{(i)})$
  $ESS = 1/\sum_{i=1}^{M} \left(\pi_k^{(i)} \right)^2$
  for $i := 1$ to M **do**
    if $ESS < ESS_{\text{th}}$ **then**
      $\boldsymbol{x}_k^{(i)} \sim \begin{cases} \tilde{\boldsymbol{x}}_k^{(1)} & \text{with prob. } \tilde{\pi}_k^{(1)} \\ \vdots & \vdots \\ \tilde{\boldsymbol{x}}_k^{(M)} & \text{with prob. } \tilde{\pi}_k^{(M)} \end{cases}$
      $\pi_k^{(i)} := 1/M$
    else
      $\boldsymbol{x}_k^{(i)} := \tilde{\boldsymbol{x}}_k^{(i)}$
    end if
  end for
  $k := k+1$
end loop

4.1 Conditions

As shown in Fig.6, a robot on the field is controlled to pass eight targets in order. Here, when the robot's estimated position reaches the distance of 0.5 [m] from a target, the current target is switched to the next target. The velocity was set constant as $v_k = 10$[m/s]. Furthermore, each parameter peculiar to the robot was defined as follows: length of wheel base is $l = 1$[m], noise parameters of velocity $\alpha_1 = \alpha_3 = \alpha_5 = 3.0$, noise parameters of steering $\alpha_2 = \alpha_4 = \alpha_6 = 0.3$, feedback gain $k_\phi = 0.8$, and the sampling period $\Delta = 0.01$[s].

Each parameter of the noise in a GPS signal was defined as follows: $\sigma_b^2 = 0.0025$, $\sigma_p^2 = 0.01$. Furthermore, it was assumed that the area of $x < 0$, i.e., half of the field, was a shadow area and the bias and variance of a Gaussian noise added to the GPS signal in the area were given as follows:

$$r_k = \begin{cases} x_k & \text{if } r_k \leq 5.0 \\ 5.0 & \text{otherwise,} \end{cases} \tag{44}$$

$$\sigma_s^2 = 0.1. \tag{45}$$

The number of particles of the PF was $M = 1000$ and $ESS_{\text{th}} = 5.0$.

Furthermore, for comparison with the proposed method, the simulation was performed using the following composition of a general PF, i.e., the sampling follows a system model:

$$\tilde{\boldsymbol{x}}_k^{(i)} \sim p_q\left(\tilde{\boldsymbol{x}}_k^{(i)} | \boldsymbol{x}_{k-1}^{(i)} \right) = p_f\left(\tilde{\boldsymbol{x}}_k^{(i)} | \boldsymbol{x}_{k-1}^{(i)} \right). \tag{46}$$

Moreover, only the likelihood function is used when the direct detection of the GPS signal can be carried out, i.e.,

$$p_h\left(\boldsymbol{y}_k^{\text{GPS}} | \boldsymbol{x}_k^{(i)} \right) = p_{\text{direct}}\left(\boldsymbol{y}_k^{\text{GPS}} | \boldsymbol{x}_k^{(i)} \right). \tag{47}$$

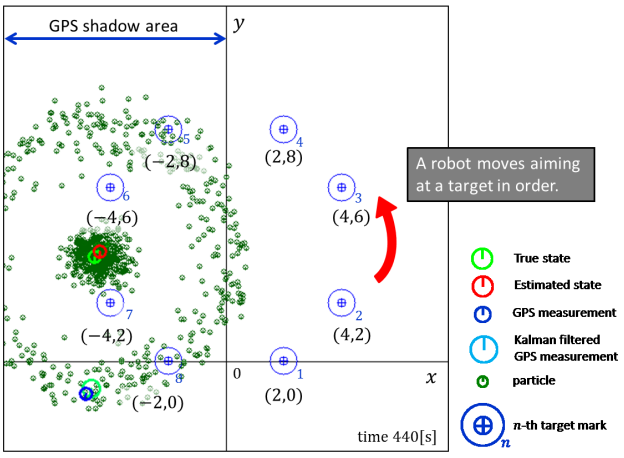

Fig. 6 Conditions of the simulation.

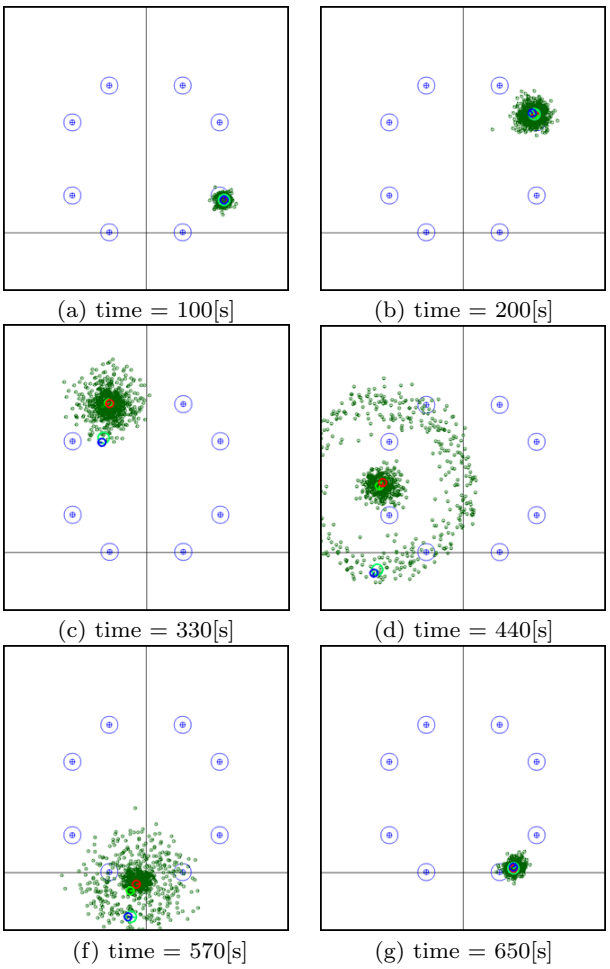

(a) time = 100[s] (b) time = 200[s]

(c) time = 330[s] (d) time = 440[s]

(f) time = 570[s] (g) time = 650[s]

Fig. 7 A part of the result of the state estimation using the proposed method and particle distribution.

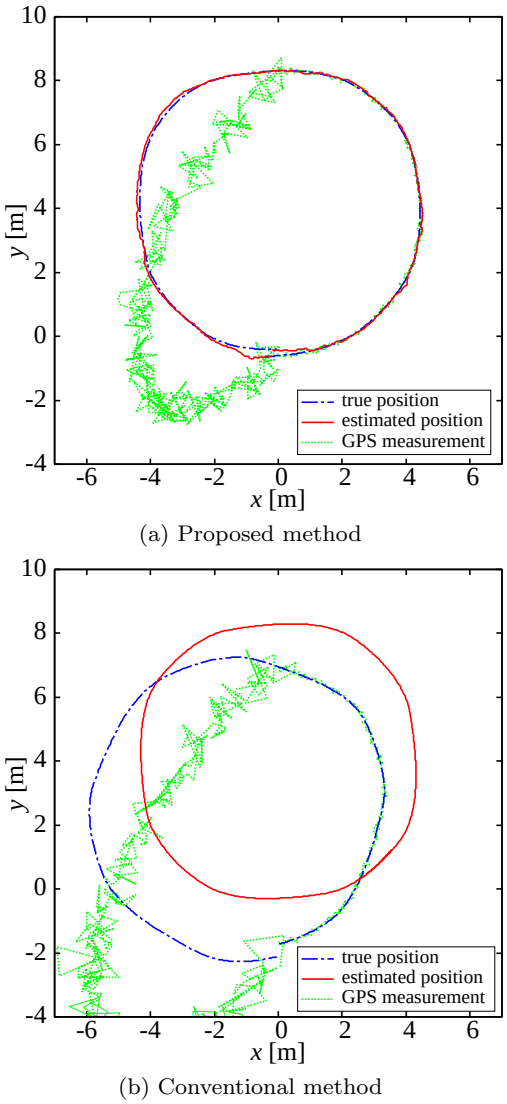

(a) Proposed method

(b) Conventional method

Fig. 8 Trajectories of the estimation, measurement, and true state values on the third track using (a) proposed method and (b) conventional method.

4.2 Results

A part of the result of the state estimation using the proposed method and particle distribution is shown in Fig.7. These figures show that particles are concentrically distributed to a true state on the basis of the value of the estimated bias in the shadow area. Next, the trajectories of the robot depended on the proposed and conventional methods one are shown in Fig.8(a) and (b), respectively. These results indicate that the state estimation in the shadow area is accurate when the proposed method is used and a suitable control method is executed. In contrast, owing to the accumulation of errors in the kinematics model, the robot deviated significantly from the target trajectory when the conventional method was used.

Furthermore, the time evolution of the estimated error of each state variable is shown in Fig.9. These results indicate that the state variables are estimated with sufficient accuracy using the proposed method. In contrast, state estimation using the conventional method became unstable with time. This is attributable to the error of state estimation being amplified by the feedback control system.

5 Conclusion

We proposed a method to improve the state estimation accuracy of mobile robots near high-rise buildings using the statistical property of reflected wave and diffracted wave of a GPS signal. First, it was assumed that GPS signal that contains reflected and diffracted waves is denoted by the sum of the true position information and noise that follows a time-varying Gaussian distribution.

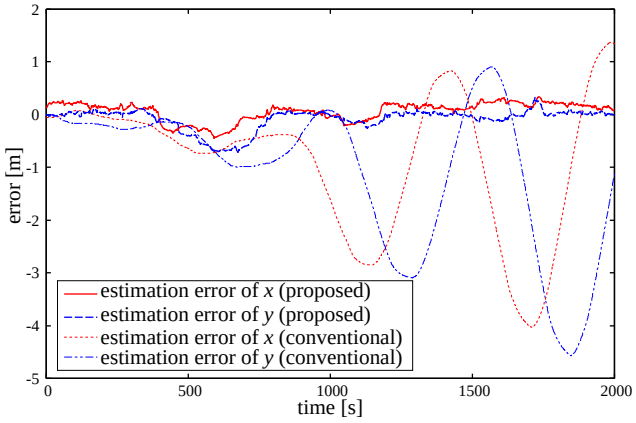

(a) Estimation error of the robot posision.

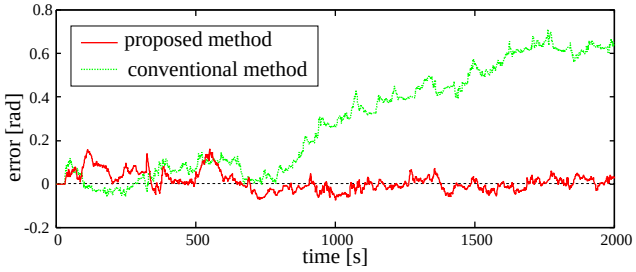

(b) Estimation error of the robot direction.

Fig. 9 Time evolution of the estimated error of each state variable.

On the basis of this assumption, a novel state observer using the KF and PF was constructed and installed into a feedback control system. Furthermore, the effectiveness of the control system for the autonomous mobile robot was shown via simulation.

For future work, the validity of the proposed method will be verified by performing experiments in an actual outdoor environment.

References

1. B. Hofmann-Wellenhof, H. Lichtenegger, and J. Collins (2001) GPS: theory and practice (fifth, revised edition), Springer, NewYork.
2. M. Yamazaki, E. Takeuchi, K. Ohono, and S. Tadokoro: " GPS Based Particle Filter Localization Method with Multipath Model using 3D-Map", JRSJ, Vol.29, No.8, pp. 702–709 2011.
3. S. Thrun, W. Burgard, and D. Fox (2005) Probabilistic Robotics. MIT Press.
4. D. Maier and A. Kleiner (2010) Improved GPS Sensor Model for Mobile Robots in Urban Terrain, Int. Conf. on Robotics and Automation.
5. G. A. Bekey (2005) Autonomous Robots: From Biological Inspiration to Implementation and Control, MIT Press.
6. G. Kitagawa (1998) Monte Carlo Filter and Smoother for Nong-Gaussian Nonlinear State Space Models, Journal of Computational and Graphical Statistics, vol. 5, pp. 1–25.
7. A. Doucet, N. Freitas, and N. Gordon (eds) (2001) sequential Monte Carlo methods in practice, Springer, New York.
8. M. Tomono (2011) Probabilistic Approaches to Localization and Mapping for Mobile Robots, JRSJ, Vol. 29, No. 5, pp. 423–426
9. P. Corke (2011) Robotics, Vision and Control Fundamental Algorithms in MATLAB, Sringer-Verlag.
10. J. S. Liu and R. Chen (1998) Sequential Monte Carlo methods for dynamic systems, Journal of the American Statistical Association, Vol. 93, No. 443, pp. 1032–1044.